Supporting Information

"All-four-in-one": a novel mercury Tellurite-Nitrate $Hg_3(TeO_3)(Te_3O_7)(NO_3)_2$ exhibiting exceptional optical anisotropy

Ru-Ling Tang*, Yi-Lei Lv, Liang Ma, Bing- Wei Miao, Wenlong Liu, Sheng-Ping Guo*

[a]School of Chemistry and Chemical Engineering, Yangzhou University, Yangzhou, Jiangsu 225002, P. R. China. *Email: rltang@yzu.edu.cn, spguo@yzu.edu.cn.*

Corresponding authors: rltang@yzu.edu.cn ; spguo@yzu.edu.cn.

Supporting Information Index

3) **Table S3.** Fractional Atomic Coordinates ($\times 10^4$) and Equivalent Isotropic Displacement Parameters ($Å^2 \times 10^3$) for $Hg_3(TeO_3)(Te_3O_7)(NO_3)_2$. U_{eq} is defined as 1/3 of the trace of the orthogonalized Uij tensor.
4) **Table S4.** The reported birefringences of inorganic nitrates.
5) **Table S5.** Summary of reported tellurium nitrates.
6) **Figure S1.** Experimental and simulated powder XRD patterns of $Hg_3(TeO_3)(Te_3O_7)(NO_3)_2$.
7) **Figure S2.** EDS image and data of $Hg_3(TeO_3)(Te_3O_7)(NO_3)_2$.
8) **Figure S3**. TG curves of $Hg_3(TeO_3)(Te_3O_7)(NO_3)_2$.
9) **Figure S4**. (a) Calculated band structure; (b) Density of states (DOS). The fermi level is set at 0 eV;
10) **Figure S5.** IR spectrum of $Hg_3(TeO_3)(Te_3O_7)(NO_3)_2$.
11) **Figure S6.** (a) Coordination geometry of $Hg_3(TeO_3)(Te_3O_7)(NO_3)_2$; (b, c, d) The arrangements of NO_3 groups in $Hg_3(TeO_3)(Te_3O_7)(NO_3)_2$.
12) **Figure S7.** The arrangement of $[(Hg_3O_7)^{8-}]_\infty$ chains; (b) The arrangement of (TeO_3) units and $[(Te_3O_7)^{2-}]_\infty$ chains.
13) **Figure S8.** The theoretical calculation birefringences in certain tellurium nitrate crystals.

EXPERIMENTAL SECTION

The raw materials include TeO_2 (HEOWNS, 4N), $Hg(NO_3)_2 \cdot H_2O$ (damas, 99%), ZnO (Aladdin, AR), and HCl (AR, 36-38%). All products are used directly without further processing. (Caution: $Hg(NO_3)_2 \cdot H_2O$ and HCl is toxic and must be handled with extreme caution, using appropriate protective equipment and training.)

Synthesis. The single crystals of $Hg_3(TeO_3)(Te_3O_7)(NO_3)_2$ were synthesized by a hydrothermal method. 0.5 mmol TeO_2 (80.4 mg), 0.49 mmol $Hg(NO_3)_2 \cdot H_2O$ (167.8 mg), 0.51 mmol ZnO (41.2 mg), fifteen drops solution, and 3 ml deionized water were poured into a 23 ml Teflon pad. The reaction temperature was set at 200 ℃ and heated at a rate of 1℃/minute from room temperature, maintained at 200 ℃ for 3 days, and then cooled down to room temperature at a rate of 2℃ per hour. The yield is about 80 % based on the mass of ZnO.

Single crystal structure determination. The crystallographic data of $Hg_3(TeO_3)(Te_3O_7)(NO_3)_2$ was collected using a Bruker D8 Electronic X-ray diffractometer equipped with graphite-monochromate Mo-Kα radiation (λ = 0.71073 Å).[1] The structure was solved through Direct Methods and refined using full-matrix least-squares techniques on F^2, incorporating anisotropic displacement parameters for all atoms. It is important to note that Te3 exists in a fragmented state, leading to the respective ratios of Te(3A) and Te(3B) being 0.9 and 0.1. After undergoing processing, there will be no warning messages displayed. The final refinement process, performed with the SHELXTL program package, included determination of the anisotropic displacement parameters for all atoms as well as correctional crystalline parameter data (Table S1). For atomic coordinates, equivalent isotropic displacement parameters, Wyckoff sites, and bond lengths are listed in Table S2 and Table S3. The single-crystal structure data was also deposited with the CCDC number 2400692.

Powder X-ray diffraction Analysis. A Bruker D8 Advance diffraction instrument with Cu-Kα radiation (λ = 1.5406 Å) conducted PXRD measurement on $Hg_3(TeO_3)(Te_3O_7)(NO_3)_2$ powder sample. The range of 2θ was 10-70 °, the step length was 0.02 °, and the scan rate per step was 1s. The simulated pattern was solved by Mercury program. The purity of the powder sample was confirmed by PXRD analysis (Figure S1).

Thermal analysis. The thermal stability of $Hg_3(TeO_3)(Te_3O_7)(NO_3)_2$ in the flow of N_2 gas was measured on the Netzsch STA 449 F3 thermal analyser. The powder sample was placed in alumina crucible and heated from 20 °C to 1000 °C at a rate of 15 °C min^{-1}.

Infrared (IR) and UV-vis-NIR diffuse reflectance spectroscopies. UV-vis-NIR diffuse reflectance spectrum of $Hg_3(TeO_3)(Te_3O_7)(NO_3)_2$ was collected on powder samples with $BaSO_4$ as standard on a Carry

5000 UV-vis-NIR spectrometer, and the spectral range is set as 200–1400 nm. IR spectrum was recorded in the range of 400 to 4000 cm^{-1} on a Fourier transform IR spectrometer.

Energy-dispersive X-ray spectroscopy. The EDS analysis was performed on several selected crystals using the Brook quantum scatter X-ray spectrum. The data proves that there are Hg, Te, N, and O in the crystal, and the proportion is close to the chemical formula (Figure S3).

Birefringence measurements. The birefringence of $Hg_3(TeO_3)(Te_3O_7)(NO_3)_2$ was measured with a polarizing light microscope (ZEISS Axio Scope A1), by means of tilting the compensator and compensating the optical path difference. The birefringence was calculated according to Eq: $R = \Delta n \times T$, where R denotes the optical path difference, Δn represents the birefringence, and T is the thickness of the crystal.[2]

Theoretical calculations. $Hg_3(TeO_3)(Te_3O_7)(NO_3)_2$ single crystal structure data provided a computing model. The CASTEP module in Material Studio software was used to calculate the structure, state density (DOS), and optical properties.[3,4] The generalized gradient approximation (GGA) by Perdew−Burke−Ernzerhof (PBE) was selected as the exchange–correlation function. The graphic wave cut-off energy was 340 eV.[5] The configurations of different electron orbitals are Hg:$6s^25d^{10}$, Te:$5s^25p^4$, N:$2s^22p^3$ and O:$2s^22p^4$. Numerical points were made for the Bourin area using a 3 × 1 × 1 Monkhorsst-Pack k point grid with a Fermi level of 0 eV as a reference.[6]

TABLES AND FIGURES

Table S1. Crystal data and structure refinement parameters for $Hg_3(TeO_3)(Te_3O_7)(NO_3)_2$.

Empirical formula	**$Hg_3(TeO_3)(Te_3O_7)(NO_3)_2$**
Formula weight	1396.199
Temperature/K	296
Crystal system	orthorhombic
Space group	*Pnma*
a/Å	9.2209(7)
b/Å	8.3046(6)
c/Å	19.3943(15)
α/°	90
β/°	90
γ/°	90
Volume/Å^3	1485.14(19)
Z	4
ρ_{calc} g/cm^3	6.244
μ/mm^{-1}	38.730
F(000)	2360.0
Crystal size/mm^3	0.10 × 0.10 × 0.09
Radiation	MoKα (λ = 0.71073)
2Θ range for data collection/°	5.336 to 50.052
Index ranges	-10 ≤ h ≤ 10,-9 ≤ k ≤ 9,-23≤ l ≤ 23
Reflections collected	16669
Independent reflections	1410 [R_{int} = 0.0645, R_{sigma} = 0.0282]
Data/restraints/parameters	1410/24/141
Goodness-of-fit on F^2	1.120
Final R indexes [I ≥ 2σ (I)] [a,b]	R_1 = 0.0318, WR_2 = 0.0561
Final R indexes [all data][a,b]	R_1 = 0.0413, WR_2 = 0.0586

[a]$R_1 = \sum||F_o| - |F_c||/\sum|F_o|$ and [b]$wR_2 = [w (F_o^2 - F_c^2)^2/wF_o^4]^{1/2}$ for $F_o^2 > 2\sigma (F_o^2)$

Table S2. Important bond lengths (Å) and bond angles (°) for $Hg_3(TeO_3)(Te_3O_7)(NO_3)_2$.

Bond length (Å)			
Hg(1)—O(1)	2.145(10)	Te(2)—O(2)[1]	2.068(7)
Hg(1)—O(3)	2.137(11)	Te(2)—O(4)	1.921(11)
Hg(1)—O(5)[1]	2.578(8)	Te(3)[1]—O(1)	1.895(11)
Hg(1)—O(5)	2.578(8)	Hg(2)[1]—O(3)	2.556(6)
Hg(1)—O(6)[2]	2.529(11)	Te(3A)—O(3)	2.21(7)
Hg(2)—O(3)	2.556(6)	Te(3)[1]—O(2)	2.068(7)
Hg(2)—O(5)	2.166(8)	Hg(1)[2]—O(6)	2.529(11)
Hg(2)—O(7)	2.480(9)	Te(1)[4]—O(6)	1.966(4)
Hg(2)—O(7)[3]	2.110(8)	Te(1)[1]—O(4)	2.349(2)
Te(1)—O(5)	1.877(8)	Te(2)[1]—O(4)	1.921(11)
Te(1)—O(2)	1.909(8)	Hg(2)[3]—O(7)	2.110(8)
Te(1)—O(6)	1.966(4)	Te(3A)—O(7)	2.18(7)
Te(1)—O(4)	2.349(2)	N(2)—O(8)	1.25(2)
Te(3)—O(3)	1.895(12)	N(2)—O(9)	1.18(2)
Te(3)—O(7)[1]	1.889(9)	N(2)—O(10)	1.26(2)
Te(3)—O(7)	1.889(9)	N(1)—O(11)	1.28(2)
Te(2)—O(1)	1.895(11)	N(1)—O(12)	1.228(13)
Te(2)—O(2)	2.068(7)	N(5)—O(12)[1]	1.228(13)
Te(3A)—O(7)[1]	2.18(7)		
Bond Angles (deg)			
O(1)—Hg(1)—O(5)	98.6 (2)	O(2)—Te(1)—O(4)	71.1 (3)
O(1)—Hg(1)—O(5)[1]	98.6 (2)	O(6)—Te(1)—O(4)	152.0 (4)
O(1)—Hg(1)—O(6)[2]	111.5 (4)	O(7)—Te(3)—O(3)	88.5 (4)
O(3)—Hg(1)—O(1)	170.1 (4)	O(7)[1]—Te(3)—O(3)	88.5 (4)
O(3)—Hg(1)—O(5)[1]	75.5 (2)	O(7)—Te(3)—O(7)[1]	102.3 (6)

O(3)—Hg(1)—O(5)	75.5 (2)	O(1)—Te(2)—O(2)	88.5 (2)
O(3)—Hg(1)—O(6)^{2}	78.4 (4)	O(1)—Te(2)—O(2)^{1}	88.4 (2)
O(5)^{1}—Hg(1)—O(5)	103.1 (4)	O(1)—Te(2)—O(4)	100.7 (5)
O(6)^{2}—Hg(1)—O(5)	120.5 (2)	O(2)^{1}—Te(2)—O(2)	153.9 (4)
O(6)^{2}—Hg(1)—O(5)^{1}	120.5 (2)	O(4)—Te(2)—O(2)^{1}	77.6 (2)
O(5)—Hg(2)—O(3)	75.5 (3)	O(4)—Te(2)—O(2)	77.6 (2)
O(5)—Hg(2)—O(7)	129.2 (3)	O(11)—N(2)—O(10)	119.4 (17)
O(7)—Hg(2)—O(3)	63.2 (3)	O(12)—N(2)—O(11)	118.4 (18)
O(7)^{3}—Hg(2)—O(3)	125.0 (3)	O(12)—N(2)—O(10)	122.3 (17)
O(7)^{3}—Hg(2)—O(5)	157.7 (3)	O(12)^{1}—N(1)—O(8)	119.2 (10)
O(7)^{3}—Hg(2)—O(7)	72.6 (3)	O(9)—N(1)—O(8)	119.2 (10)
O(5)—Te(1)—O(6)	95.9 (3)	O(9)^{1}—N(1)—O(9)	121.6 (19)
O(5)—Te(1)—O(6)	88.3 (4)	O(7)^{1}—Te(3A)—O(3)	74 (3)
O(5)—Te(1)—O(4)	84.9 (4)	O(7)—Te(3A)—O(3)	74 (3)
O(2)—Te(1)—O(6)	82.7 (4)	O(7)—Te(3A)—O(7)^{1}	85 (3)

Symmetry transformations used to generate equivalent atoms: ^{1}+*x*, 1/2-*y*,+*z*; ^{2}1-*x*, 1-*y*, 1-*z*; ^{3}2-*x*, 1-*y*, 1-*z*; ^{4}+*x*, 3/2-*y*, +*z*

Table S3. Fractional Atomic Coordinates (× 10^4) and Equivalent Isotropic Displacement Parameters (Å^2 × 10^3) for $Hg_3(TeO_3)(Te_3O_7)(NO_3)_2$. U_{eq} is defined as 1/3 of the trace of the orthogonalized U_{ij} tensor.

atom	Wyckoff site	*x*	*y*	*z*	U_{eq}[a]/Å^2
Hg1	4*c*	5080.9(7)	2500	5006.8(4)	14.01(18)
Hg2	8*d*	8262.0(5)	5052.8(6)	5478.9(3)	21.69(16)
Te1	8*d*	5123.5(8)	5283.0(9)	6585.1(4)	13.7(2)
Te2	4*c*	2667.0(12)	2500	6300.2(6)	13.0(3)
Te3	4*c*	8498(3)	2500	4053(4)	9.1(9)
O1	4*c*	2855(11)	2500	5327(5)	13(3)
O3	4*c*	7382(12)	2500	4873(6)	15(3)
O5	8*d*	5970(8)	4931(10)	5718(4)	17.3(18)
O2	8*d*	3172(8)	4926(9)	6293(4)	15.0(17)
O6	4*c*	4699(12)	7500	6293(6)	12(2)
O6	4*c*	4671(12)	2500	6572(7)	19(3)
O7	8*d*	9545(9)	4272(11)	4406(5)	28(2)
N2	4*c*	8282(17)	7500	7005(9)	27(4)
O11	4*c*	9622(15)	7500	7103(8)	54(5)
O12	4*c*	7513(18)	7500	7488(8)	64(5)
O10	4*c*	7801(15)	7500	6396(7)	38(4)
N1	4*c*	3239(19)	2500	8142(10)	33(4)
O8	4*c*	3870(17)	2500	8727(8)	41(4)
O9	8*d*	2949(13)	3791(13)	7866(6)	52(3)
Te3A	4*c*	8310(60)	2500	3820(50)	19(9)

Table S4. The reported birefringence of inorganic nitrates. ("Exp." means the experimental value, "Cal." means the calculate value)

Compound	**Space group**	**Birefringence**	**Reference**
$Sc(IO_3)_2(NO_3)$	*R*32	Exp.0.348@546nm	7a
$Pb_6O_4(BO_3)(NO_3)$	*Pmmn*	Cal.0.276@546nm	19a
$In(IO_3)_2(NO_3)$	*R*32	Cal.0.268@546nm	19b
$[Al(H_2O)_6](IO_3)_2(NO_3)$	$P\bar{3}m1$	Cal.0.252@546nm	19c
$Pb_6O_2(BO_3)_2(NO_3)F$	$P2_1$/m	Cal.0.241@546nm	19a
$Pb_2(NO_3)_2(H_2O)F_2$	*Amm*2	Cal.0.230@1064nm	19d
$Hg_3O_2(NO_3)F$	*Pbca*	Cal.0.230@1064nm	18b
$[In(IO_3)(OH)(H_2O)](NO_3)$	$P2_1/n$	Cal.0.188@532nm	19b
$Pb_2(BO_3)(NO_3)$	$P6_3mc$	Cal.0.174@1064nm	12
$Hg_{16}O_{12}(NO_3)_6F_2(H_2O)$	*Ibca*	Exp.0.17@546nm	19e
$(NH_4)_3SbF_4(NO_3)_2$	*Pnma*	Exp.0.164@546nm	19f
$Bi(SO_4)(NO_3)\cdot 3H_2O$	$P2_1/m$	Cal.0.163@546 nm	7b
$Cs_2Pb(NO_3)_2Br_2$	$I4_1/amd$	Exp.0.147@546nm	19g
$La(OH)_2NO_3$	$P2_1$	Exp.0.146@589.6nm	19h
$CsHgNO_3Cl_2$	$P6_3/mmc$	Exp.0.145@ 546nm	19i
$Na_3Rb_6(CO_3)_3(NO_3)_2Cl\cdot(H_2O)_6$	$P6_3/mcm$	Exp. 0.14@546nm	7c
$Y(OH)_2NO_3$	$P2_1$	Exp.0.133@589.6nm	19h
$Bi_3TeO_6OH(NO_3)_2$	$P2_1$	Cal.0.115@1064nm	13
$Gd(OH)_2NO_3$	$P2_1$	Exp.0.112@589.6nm	19h
$K_2Hg(NO_3)_4$	$I\bar{4}2m$	Exp.0.107@546nm	18a
$Rb_2Hg(NO_3)_4$	$I\bar{4}2m$	Exp.0.092@546nm	18a
$(NH_4)_3SbF_3(NO_3)_3$	$P2_1$	Exp.0.098@546nm	7d
$Ba_2NO_3(OH)_3$	$P\bar{6}2m$	Cal.0.082@532nm	7e
$Sr(NO_3)(NH_2SO_3)\cdot H_2O$	$Pca2_1$	Cal.0.0665@532nm	7f

$Rb_2SbF_3(NO_3)_2$	$P2_1$	Cal.0.06@1064nm	19h
$PbCdF(SeO_3)(NO_3)$	$Pca2_1$	Cal.0.055@1064nm	7g
$RbSnF_2NO_3$	$C2/m$	Cal.0.05@1064nm	19h
$Bi_2O_2(OH)(NO_3)$	$Cmc2_1$	Cal.0.045@1064nm	7h
$Na_{10}Zn(NO_3)_4(SO_3S)_4$	$P\bar{4}$	Exp.0.013@550nm	7i
$Na_{10}Cd(NO_3)_4(SO_3S)_4$	$P\bar{4}$	Cal.0.01@1064nm	7j

Table S5. Summary of reported tellurite nitrate compounds. ("—" means no data available)

Compounds	Space group	Dimension	Birefringence	Tellurium atomic manifestation
$(SbTeO_3)(NO_3)$	$Pca2_1$	2D	Exp.0.078@546 nm	TeO_3 unit
$Ca_5Te_4O_{12}(NO_3)_2(H_2O)_2$	Cc	0D	——	TeO_3 unit
$Ca_6Te_5O_{15}(NO_3)_2$	$P2_1/c$	3D	——	TeO_3 unit
$Bi_3(\mu_3\text{-}OH)(TeO_3)_3(NO_3)_2$	$P\bar{6}2m$	1D	——	TeO_4 unit, $[(Te_3O_{10})^{8-}]_\infty$ chain
$AgTeO_2NO_3$	$Pbcn$	2D	——	$(TeO_2)_\infty$ chain
$[Bi(TeO_3)](NO_3)$	$P2/c$	2D	——	TeO_3 unit
$(Te_2O_4)(HNO_3)$	$Pnma$	2D	——	TeO_4 unit, Te_2O_2 ring
$H[Bi_3O(Te_3O_9)](NO_3)_2$	$P\bar{6}2m$	1D	——	$[(TeO_4)^{4-}]_\infty$ chain
$YCu(TeO_3)_2(NO_3)(H_2O)_3$	$P2_1/c$	2D	——	TeO_3 unit
$RE(TeO_3)(NO_3)$ (RE= La and Nd)	$P2_1/n$	2D	——	TeO_3 and TeO_4 units
$RE(TeO_3)(NO_3)$ (RE= Eu, Gd, Dy, Er, and Y)	$Cmca$	2D	——	TeO_3 and TeO_4 units

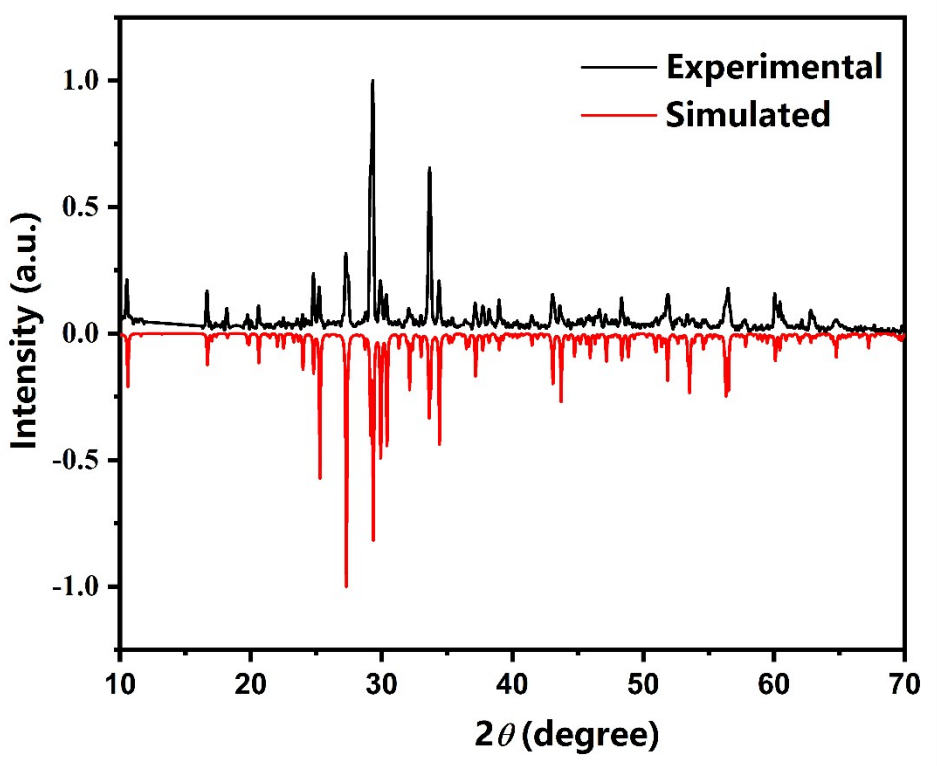

Figure S1. Experimental and simulated powder XRD patterns of $Hg_3(TeO_3)(Te_3O_7)(NO_3)_2$.

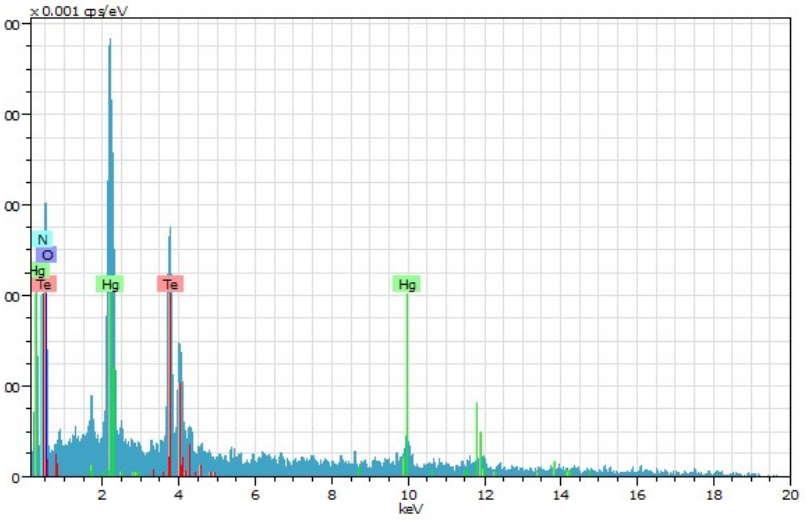

The molar ratio of Hg : Te : O : N from the EDS results.

		Molar ratio
1	Hg : Te : O : N	11.93 : 16.62 : 7.95 : 63.5=1.5 : 2.1 : 1 : 7.99
2	Hg : Te : O : N	11.86 : 16.2 : 8.7 : 63.3=1.5 : 2.05 : 1.1 : 8
3	Hg : Te : O : N	12.1 : 16.15 : 8.1 : 63.65=1.5 : 2 : 1 : 7.89

Figure S2. EDS image and data of $Hg_3(TeO_3)(Te_3O_7)(NO_3)_2$.

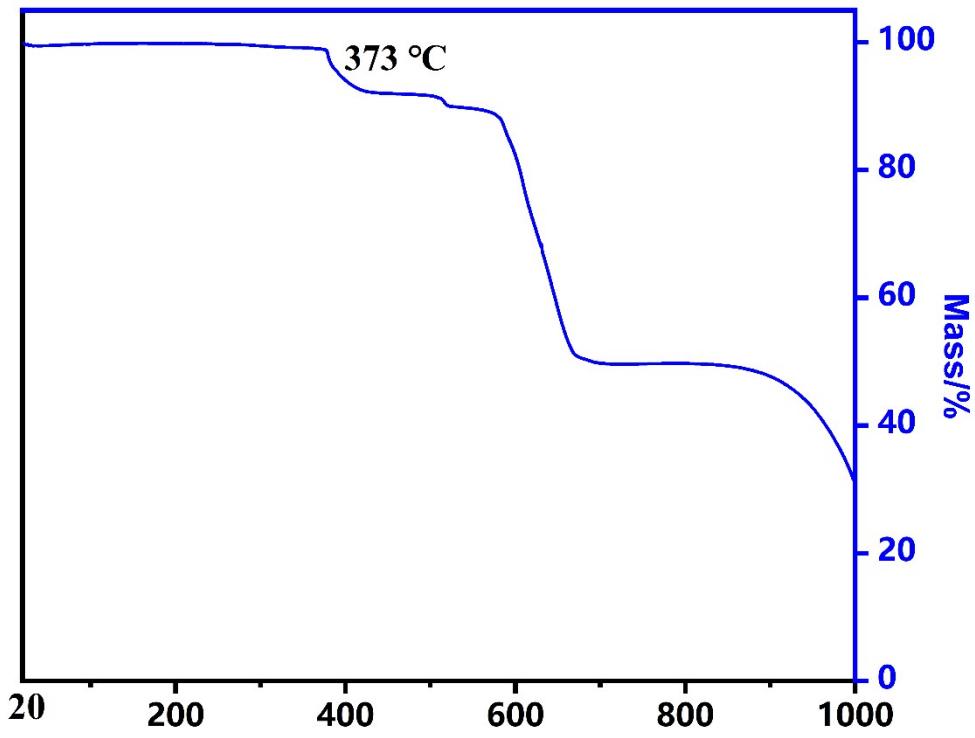

Figure S3. TG of $Hg_3(TeO_3)(Te_3O_7)(NO_3)_2$.

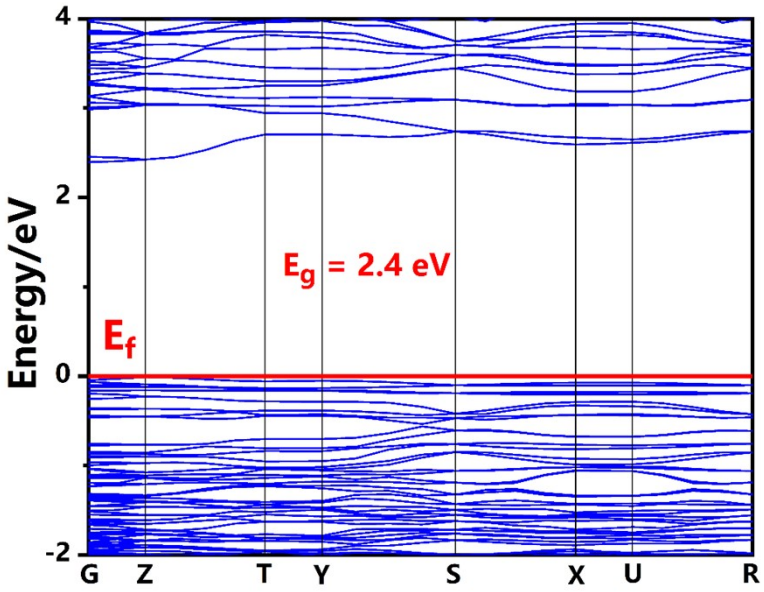

(a)

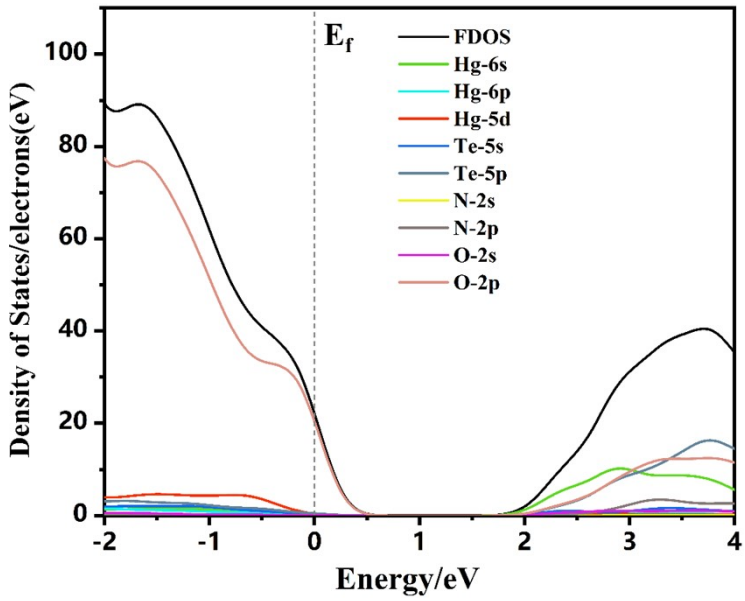

(b)

Figure S4. (a) Calculated band structure; (b) Density of states (DOS). The fermi level is set at 0 eV;

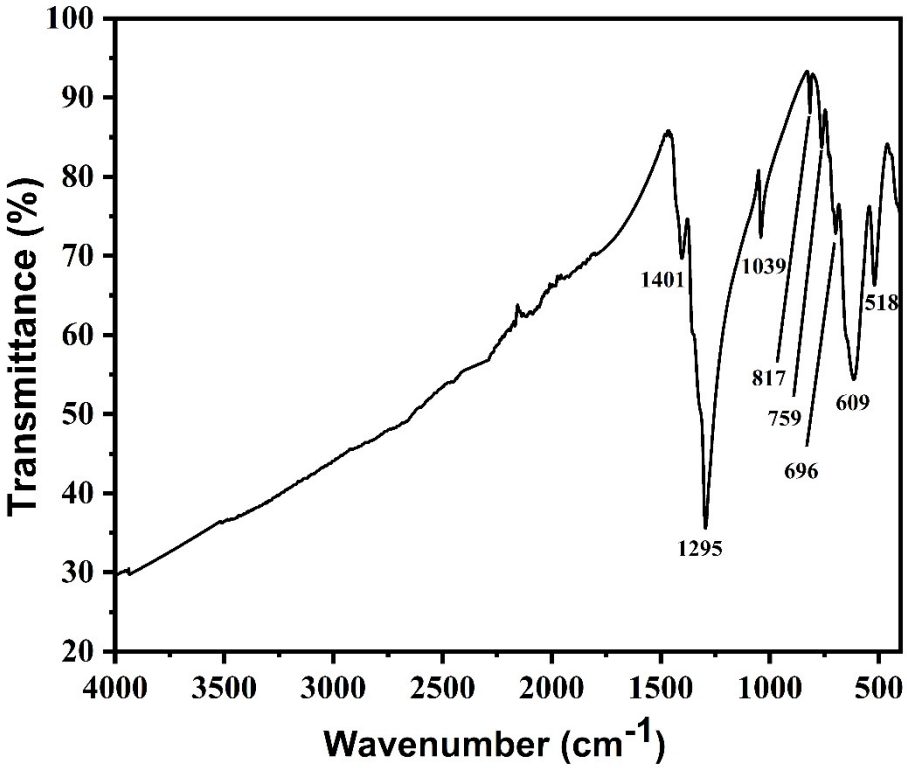

Figure S5. IR spectrum of $Hg_3(TeO_3)(Te_3O_7)(NO_3)_2$.

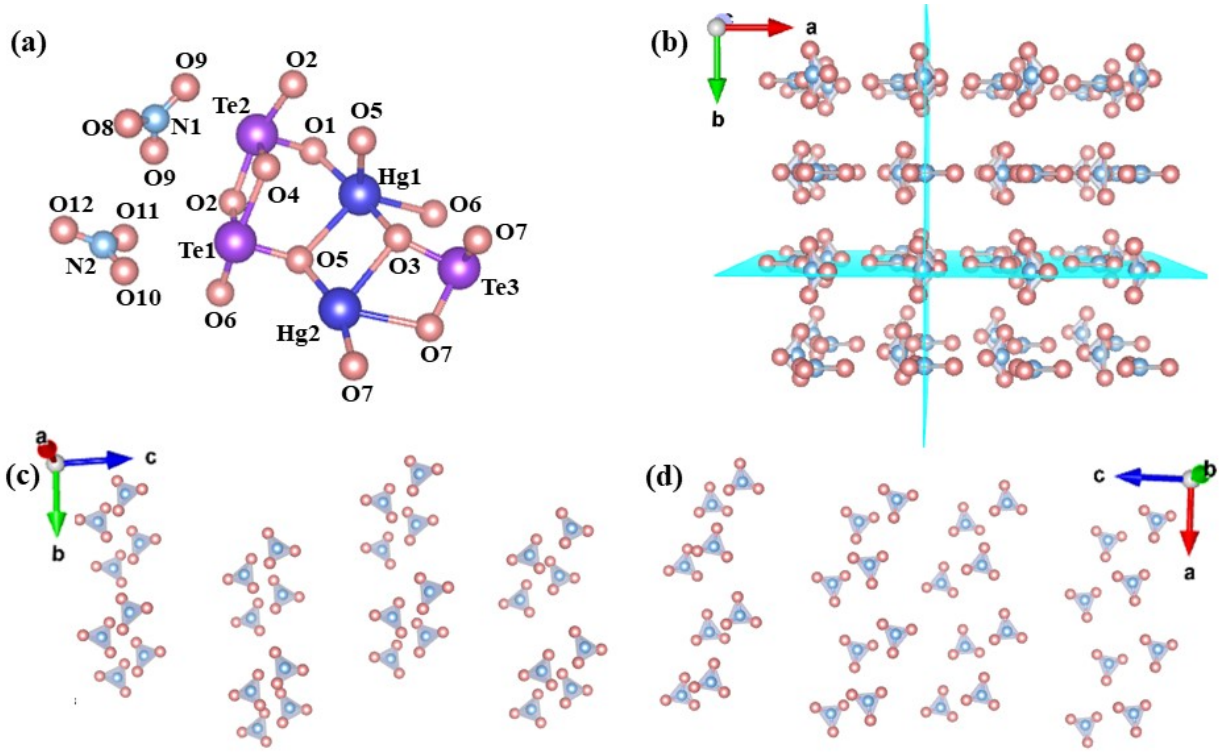

Figure S6. (a) Coordination geometry of $Hg_3(TeO_3)(Te_3O_7)(NO_3)_2$; (b, c, d) the arrangements of NO_3 groups in $Hg_3(TeO_3)(Te_3O_7)(NO_3)_2$.

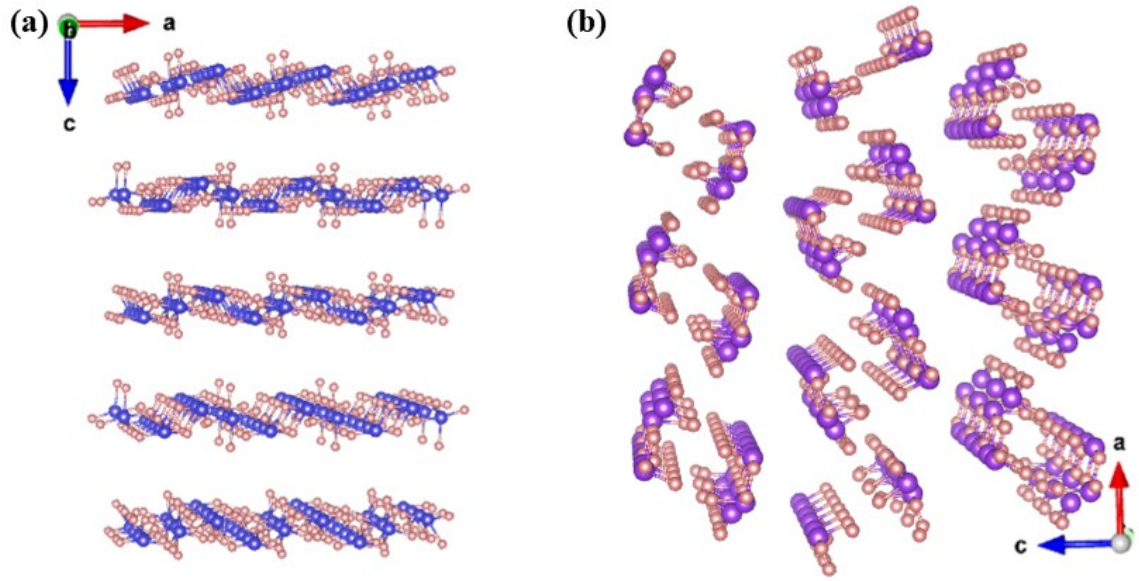

Figure S7. The arrangement of $[(Hg_3O_7)^{8-}]_\infty$ chains; (b) The arrangement of (TeO_3) units and $[(Te_3O_7)^{2-}]_\infty$ chains.

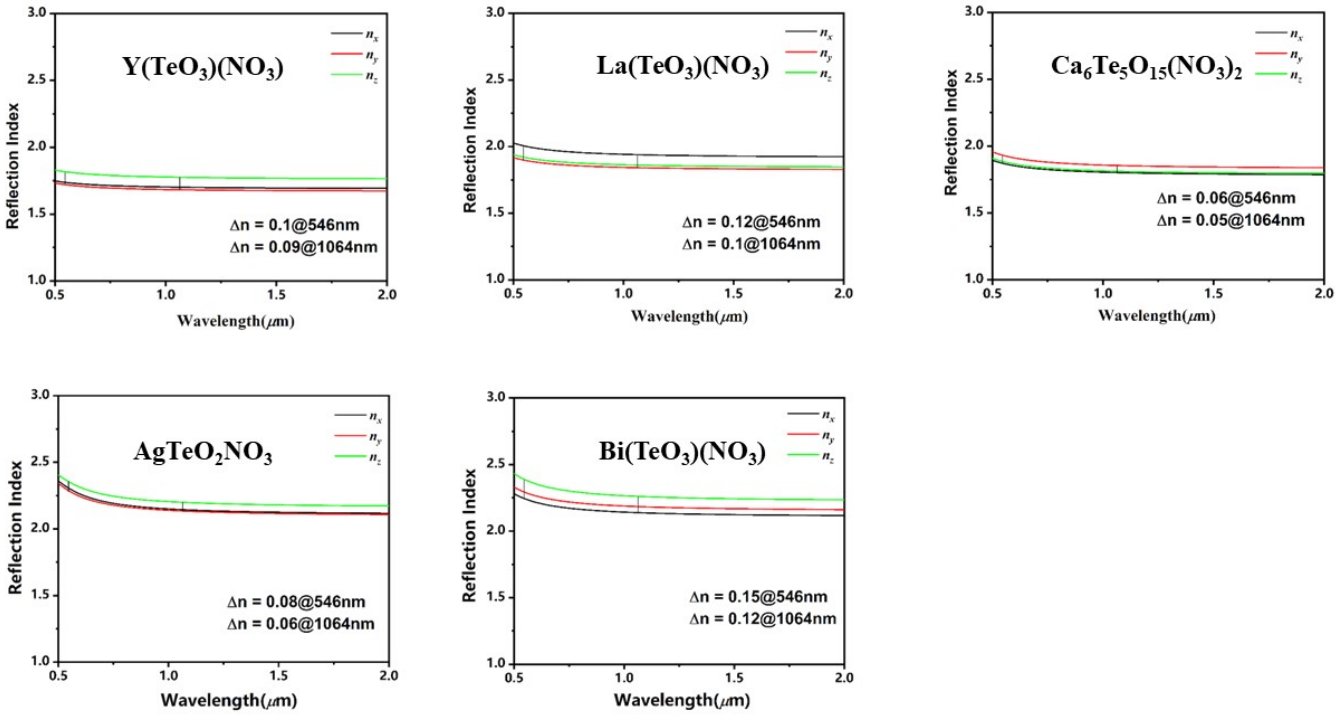

Figure S8. The theoretical calculation values of birefringence in certain tellurium nitrate crystals.

References:

[1] V. Dolomanov, L. J. Bourhis, R. J. Gildea, J. A. K. Howard, H. Puschmann, *J. Appl. Crystallogr.,* 2009, **42**, 339–341.

[2] J. Chen, M. B. Xu, H. Y. Wu, J. Y. Wu, K. Z. Du, *Angew. Chem. Int. Ed.,* 2024, **63**, e202411503.

[3] M. D. Segall, P. J. D. Lindan, M. J. Probert, C. J. Pickard, P. J. Hasnip, S. J. Clark, M. C. Payne, *J. Phys. Condens. Mat.,* 2002, **14**, 2717.

[4] J. C. Stewart, D. S. Matthew, J. P. Chris, J. H. Phil, I. J. P. Matt, R. Keith, C. P. Mike, Z. Kristallogr, *Cryst. Mater.,* 2005, **220**, 567–570.

[5] J. Paier, M. Marsman, K. Hummer, G. Kresse, I.C. Gerber, J. G. Ángyán, *J. Chem. Phys.,* 2006, **124**, 154709.

[6] X. Huang, S. H. Yang, X. H. Li, W. L. Liu, S. P. Guo, *Angew. Chem. Int. Ed.,* 2022, **61**, e202206791.

[7] a) C. Wu, X. X. Jiang, Z. J. Wang, L. Lin, Z. S. Lin, Z. P. Huang, X. F. Long, M. G. Humphrey, C. Zhang, *Angew. Chem. Int. Ed.,* 2021, **60**, 3464-3468; b) J. C. Lu, Y. Li, Y. Kuk, S. Choi, K. Kim, C. Ko, Z. Y. Bai, K. M. Ok, *Inorg. Chem.,* 2024, **63**, 13748–13754; c) M. Cheng, W. Q. Jin, Z. H. Yang, S. L. Pan, *Chem. Sci.,* 2022, **13**, 13482-13488; d) X. H. Dong, L. Huan, Q. Y. Liu, H. M. Zeng, Z. Lin, D. G. Xu, G. H. Zou, *Chem. Commun.,* 2018, **54**, 5792-5795; e) X. F. Wang, Y. Li, Z. L. Chen, J. Lee, F. F. Zhang, K. R. Poeppelmeier, S. L. Pan, K. M. Ok, *Small Struct.,* 2023, **4**, 2300274; f) L. Wang, H. M. Wang, D. Zhang, D. J. Gao, J. Bi, L. Huang, G. H. Zou, *Inorg. Chem. Front.,* 2021, **8**, 3317-3324; g) Y. X. Ma, C. L. Hu, B. X. Li, F. Kong, J. G. Mao, *Inorg. Chem.,* 2018, **57**, 11839–11846; h) T. Y. Liu, L. Hao, L. Q. Bai, J. G. Liu, Y. H. Zhang, N. Tian, H. W. Huang, *Chem. Eng. J.,* 2022, **429**, 132268; i) Z. H. Yu, Q. R. Ding, Y. H. Jiang, W. Q. Huang, C. S. Yang, S, G, Zhao, J. H. Luo, *Inorg. Chem. Front.,* 2024, **11**, 107-113; j) Y. C. Liu, Y. Q. Liu, Z. S. Lin, Y. Q. Li, Q. R. Ding, X. Chen, L. Li, S. G. Zhao, M. C. Hong, J. H. Luo, Nonpolar $Na_{10}Cd(NO_3)_4(SO_3S)_4$ Exhibits a Large Second-Harmonic Generation, *CCS Chem.*, 2022, **4**, 526–531.